History of Medicine, 2023, 9(1): 1083–1092
DOI: 10.17720/2409-5834.v9.1.2023.128

SYNTHESIS, CHARACTERIZATION AND ANTIOXID STUDY OF NEW 4-({2-[5-(2-Hydroxyphenyl)-1,3,4-Oxadiazol-2-Yl] Hydrazinylidene} Methyl)-2-Methoxy Phenol AND THEIR TRANSITION METAL COMPLEXES

Safaa H. Nasir[1*], Ibrahim A. Flifel[2]

[1] Department of Chemistry, College of Science, University of Thi-Qar, Thi-Qar, 64001, Iraq
EM: safaahakee.ch@sci.utq.edu.iq
[2] Department of Chemistry, College of Science, University of Thi-Qar, Thi-Qar, 64001, Iraq
EM: Ibrahimflifel2017@gmail.com

*Corresponding author: Safaa H. Nasir (safaahakee.ch@sci.utq.edu.iq)

Received: 20 January 2023 **Accepted:** 15 April 2023

Citation: Nasir SH, Flifel IA (2023) SYNTHESIS, CHARACTERIZATION AND ANTIOXID STUDY OF NEW 4-({2-[5-(2-Hydroxyphenyl)-1,3,4-Oxadiazol-2-Yl] Hydrazinylidene} Methyl)-2-Methoxy Phenol AND THEIR TRANSITION METAL COMPLEXES. History of Medicine 9(1): 1083−1092. https://doi.org/10.17720/2409-5834.v9.1.2023.128

Abstract

New ligand 4-({2-[5-(2-hydroxyphenyl)-1,3,4-oxadiazol-2-yl] hydrazinylidene} methyl)-2-methoxy phenol. (L) and its transition metal ion complexes Ni (II), Fe (III), Co (II), Cr (III) Cu (II) were synthesized. The authenticity of the ligand and its transition metal complexes were established by mass spectra, conductance measurements 1HNMR, FTIR, as well as elemental analyses, the program of Hyper chem 7.51 has been used up for theoretical accounts using the PM3 method to study the electrostatic potential that provided good information about the complexity site. We can suggest octahedral geometrics for Cr3+ and Fe3+ complexes, tetrahedral geometry for Ni +2 and Co+2 complex, and square planer geometry for Cu+2 the complex The ligand was tested antioxidant. the synthesized ligand showed good antioxidant, activity.

Keywords
Oxadiazole ,Ligand, Transitions metal complexes, Antioxidant

in the early nineteenth century, the chemistry of heterocyclic compounds quickly took off with the help of methods for organic synthesis. The largest area of organic chemistry is heterocyclic molecules, which have a broad variety of therapeutic applications [(1)]. Oxadiazole is a heterocyclic chemical with two nitrogen atoms and one oxygen atom in the five-member ring. It is one of several groups of heterocyclic that are particularly significant. The Oxadiazoles are comprised of many isomeric forms, such as 1,2,5, 1,2,4, 1,2,3, and 1,3,4-oxadiazoles [(2)], as illustrated in the following Figure (1)

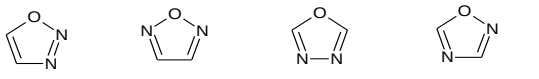

Figure (1)

The 1,3,4-oxadiazole heterocyclic compound has frequently been used as a privileged scaffold to produce a variety of novel pharmaceutical drugs, such as anti-inflammatory [(3)], antimicrobial [(4)], antiviral [(5)], antitumor [(6)], antidepressant [(7)], anthelmintic [(8)], analgesic [(9)], anti-hypoglycemic [(10)], anti-osteoporotic[(11)], anti-gastrocolic [(12)], anticancer [(13)], anti-HIV[(14)] antioxidant[(15)], analgesic[(16)] antibacterial [(17,18)],

antifungal [19] anticancer[20], anticonvulsant [21] anti-tubercular [22], lipid peroxidation inhibitor[23] and anti-diabetic [24] .1,3,4-Oxadiazole has further uses as an insecticide [9] as well as in fluorescent and colorimetric chemical sensors [25], polymers [26], and light-emitting diodes [27]. In addition to their employment as beneficial corrosion inhibitors and metal chelating agents [28], 1,3,4-oxadiazoles also have essential structural motifs in cyanine dyes [29].

Experimental

All the chemicals and solvents utilized were readily available and chemically pure. all metal salts were employed as chlorides.

Physical Measurements

An electro-thermal melting point device model (Melting SMP31) was used to calculate the melting points of the ligand and metal complexes. Using a Shimadzu FTIR spectrophotometer (Model: IR- affinity, Shimadzu), the FTIR spectra were recorded as a potassium bromide (KBr) disc for the ligand and metal complex. Utilizing a Bruker DXR System AL500 (500 MHz), TMS was utilized as the standard, and DMSO-d^6 was used as the solvent, ^{1}HNMR, Spectra. Mass Spectra (MS) were used to calculate molecular weights, which were registered in the range of 0 to 800. The results were acquired using the (Network Mass Selective Detector 5973).

Synthesis of the ligand (L)

Step I: "Synthesis of 2-hydroxy benzo hydrazide" (A) Methyl 2-hydroxybenzoate (13 ml, 0.1 mol), hydrazine hydrate (10 ml, 0.2 mol), and 100 ml of 100% ethanol were gently combined and heated under reflux for 6 hours. The product was filtered, then 2-hydroxybenzohydrazide (A) was produced by washing it with ethyl alcohol and drying it. (m.p:111- 120 C) .

Step II: "Synthesis of 2-(5-sulfanyl-1,3,4-oxadiazol-2-yl) phenyl (B)"

Potassium hydroxide (4.5 g, 0.08 mol) was heated with compound (A) (12.5 g, 0.08 mol) in 100 ml of 100% ethanol until the potassium hydroxide was entirely dissolved. The mixture was placed in ice until it reached a temperature of 0°C, at this point carbon di sulfide (5 ml, 0.08 mol) was added. For 36 hours, the mixture was heated under reflux. The product mixture was cautiously acidified with hydrochloric acid HCl (10%) and concentrated to half volume to white crystals [30] (B).

Step III: "Synthesis of 2-(5-hydrazinyl-1,3,4-oxadiazol-2-yl) phenol (C)"

Compound B (9.7 g, 0.05 mol) and hydrazine hydrate (5 ml, 0.1 mol) are combined with 50 ml of ethanol and then allowed to reflux for 42 hours. The raw material was compressed to half its original volume, then cooled [31,35-49]. The product (2-(5-hydrazinyl-1,3,4-oxadiazol-2-yl) phenol) (C) was produced by recrystallizing the crude product with ethanol. It has a yield of 64% and a melting point of 220 $C^{0.}$

Step IV: "4-({2-[5-(2-hydroxyphenyl)-1,3,4-oxadiazol-2-yl] hydrazinylidene} methyl)-2-methoxyphenol"

L) (1.92 g, 0.01 mol) of compound (C) and (1.52 g, 0.01 mol) of (4-hydroxy-3-methoxybenzaldehyde) were combined, and they were dissolved in 50 ml of 100% ethanol. also had a four-hour reflux the solution is reduced to half its original volume, and the ligand is precipitated, filtered, and recrystallized with ethyl alcohol to provide use white ligand with a melting point of 222-226 C^o and a yield of 75%. the scheme (1)

2.3 "Synthesis of complexes"

The complexes were made by mixing (0.66 g,0.002 mol)of the ligand and (0.002 mol) of each of the salts ($CrCl_3.6H_2O$, $eCl_3.6H_2O$ $CoCl_2.6H_2O$, $NiCl_2.6H_2O$, and $CuCl_2.6H_2O$) in 15 ml of ethanol and refluxing for 2 hours The resulting crystals were then filtered and occasionally washed with ethyl alcohol to remove unreacted salts or the ligand, and precipitated complexes were dried at room temperature(32).

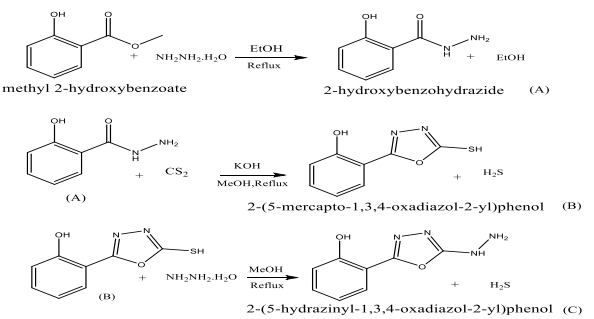

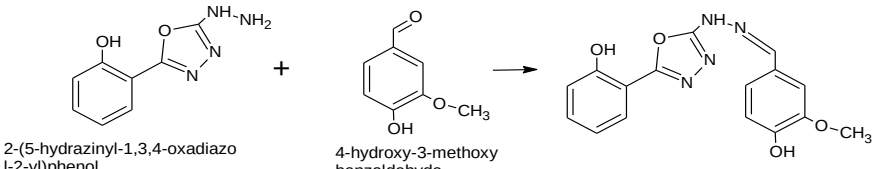

scheme (1) "Synthesis of the ligand (L)"

Table (1) Physical features of the ligand and its complexes

Num.	formula	color	M(g/mol)	M.P °C	ʌ s cm2 mol-1
1	$C_{16}H_{14}N_4O_4$	white	326	222-224	----------
2	$C_{16}H_{14}N_4O_4Cl_2Cu$	black	460	220	14.3
3	$C_{16}H_{14}N_4O_4C_{12}Ni$	Gray	455	208-210	15.7
4	$C_{32}H_{29}Cl_3N_8O_8Cr$	yellow	811	202-204	36.2
5	$C_{16}H_{14}N_4O_4Cl_3Fe$	white	488	204-206	17.6
6	$C_{32}H_{28}Cl_2O_8N_8Co$	Browne	782	210-2012	19.4

Result and Discussion

The prepared ligand and its metal complexes were characterized based on the infrared spectrum (FTIR), H1 NMR, CHN, and mass spectrum results.

3.1 Mass spectra: Mass spectra of the prepared ligand and its transition metal complex were recorded at a temperature of the room, the mass spectra of the ligand showed a molecular ion peak at 326 m/z which is by the molecular formula $[C_{16}H_{14}N_4O_4\ ]^{+\cdot}$, other peaks are due to the subsequent fragments such as (193 m/z,165 m/z,135 m/,120 m/z,106 m/z, 77m/z)respectively$[C_9H_{11}N_3O_2]^+$ [$C_8H_{10}N_2O_2]^+$, $[C_7H_7NO_2]^+$,$[C_7H_8N_2]^+$ $[C_7H_7O]^+$,$[C_6H_6]^+$.

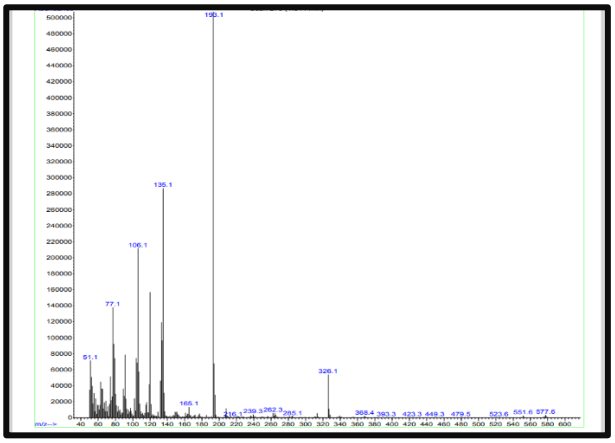

Figure (2) MS spectra of ligand

3.1.1 The MS of the complex [Ni (L) Cl_2] shows a molecular ion peak [M0] at 455 m/z that is equivalent to the molecular mass of the complex. The other peaks are shown as follows.

1- [Ni (L) Cl] $^+$ = 420 m/z
2- [Ni (L)] $^+$ = 385 m/
3- [L] $^+$ =326 m/z

3.1.2 The MS of the complex [Cu(L) Cl_2] shows a molecular ion peak at 460 m/z, The other peaks are shown as follows

4- [Cu (L) Cl] + = 425 m/z
5- [Cu (L)] + = 389 m/z
6- [L] + =326 m/z

3.1.3 The complex [$Co(L)_2$ Cl_2] showed a molecular ion peak at [M0] = 782 m/z which is equivalent to the molecular mass of the complex The other peaks are shown as follows

7- [Co (L)2Cl] + = 747 m/z
8- [Co (L)2] + =711 m/z
9- [Co (L)] + = 385 m/z
10- [L] + = 326 m/z

3.1.4 The complex [Fe(L) Cl_3] showed a molecular ion peak at [M0] = 488 m/z which is equivalent to molecular mass of the complex. The other peaks are shown as follows.

11- [Fe (L) Cl2] + = 453 m/z
12- [Fe (L) Cl] + = 417 m/z
13- [Fe (L)] + =382 m/z
14- [L] + = 326 m/z

3.1.5 The complex [Cr $(L)_2$ Cl_2] Cl showed a molecular ion peak at [M0] = 810 m/z which is equivalent to molecular mass of the complex. The other peaks are shown as follows.

15- [Cr (L)2 Cl2] = 775 m/z
16- [Cr (L)2 Cl] = 740 m/z
17- [Cr (L)2] = 704 m/z
18- [Cr (L)] = 364 m/z

19- [L] = 326 m/z

3.2 Nuclear Magnetic Resonance Spectra (^{1}H-NMR) The 1HNMR spectra data of the 2-[(Z)-{2-[5-(2-hydroxyphenyl)-1,3,4-oxadiazol-2-yl]hydrazinylidene}methyl]-6-methyl phenol, was distinguished by the appearance of multiple peaks at (2.52 and 3.40 ppm) the first due to protons of the solvent (DMSO) and the second for the D2O, (3.76 ppm, 3 H) due to protons of methoxy group, (14.05 ppm) due to N-H proton (6.92 -7.42 ppm, m, 7H) due to protons of aromatic rings, 9.24 ppm, 1 H) due to proton of azo methane group (-N=CH-), (10.00 ,10.07 ppm, s,2H) due to OH group , (14.05 ppm) due to NH proton ,as shown in figure (3)

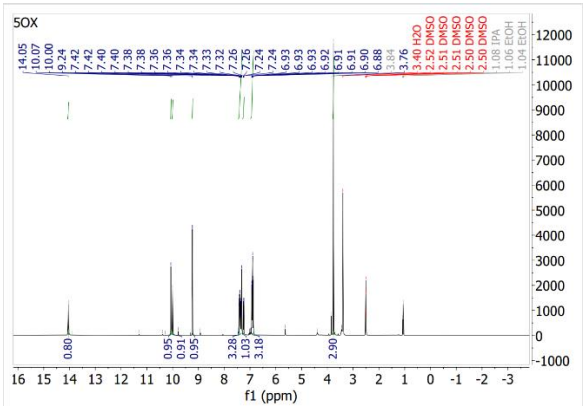

Figure (3) 1HNMR spectra of ligand

IR Spectra

FTIR spectrum of prepared ligand (L) was characterized by the presence of major absorption bands at (3248), (3200), (3038), (1584), (1476), (1518), (1254) and (1291) cm ^{1}. Which is following (υO-H), (υNH), (υArC-H), (υC=N) oxo, (υC=N) endo, (υC=C), (υC-O-C) sym, (υ C-O-C) asy bands respectively as shown in below in table (2) and figure (9). New bands were formed according to the coordinated (M- N), bond and seemed at the region () cm-1. that indicates that the coordinate occurred through (N),

Table (2) IR Measurements

compound	L2	CO	Ni	Cu	Fe	Cr
OH	3248	3245	3247	-	3255	3248
NH	3200	3121	3200	-	3134	3175
Ar (C-H)	3038	-	-	3064	3035	3037
Elf (C-H)	2954	2953	2924	2921	2950	2953
(C=N) Azo	1584	1585	1583	1597	1586	1585
(C=C)	1518	1521	1516	1509	1514	1521
(C=N) Het	1476	1491	1475	1472	1485	1472
Asy(C-O-C)	1291	1292	1289	1291	1290	1292
Sym(C-O-C)	1254	1253	1253	1252	1254	1255
Structural movement	1034	1034	1031	1027	1032	1035
M-N	-	607	632	606	611	579
M-O	-	-	-	-	458	-

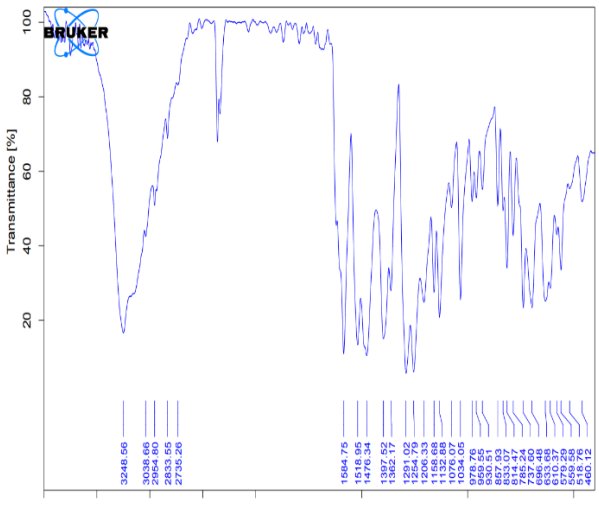

Figure (4) IR spectra of ligand

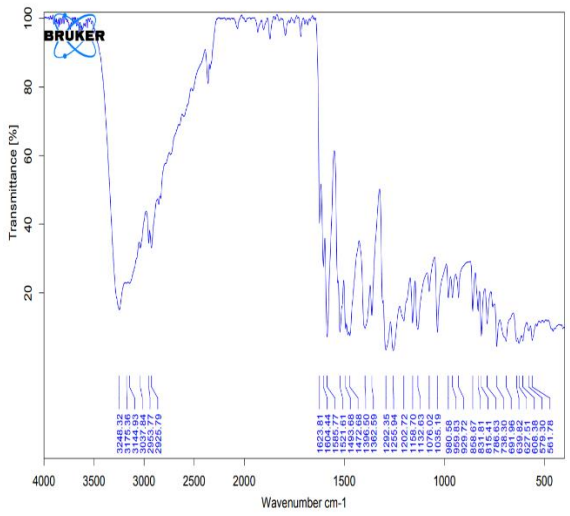

Figure (5) IR spectra of Cr complex

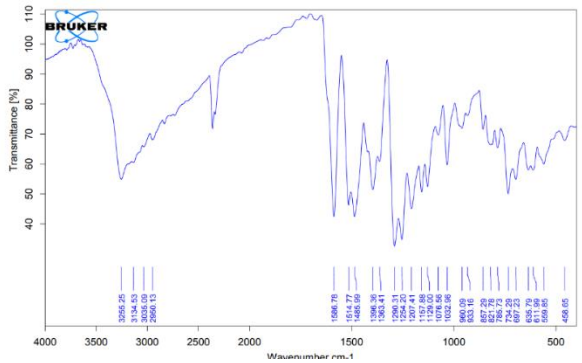

Figure (6) IR spectra of Fe Complex

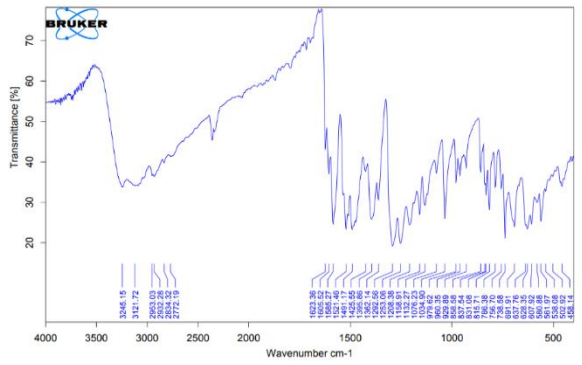

Figure (7) IR spectra of Co complex

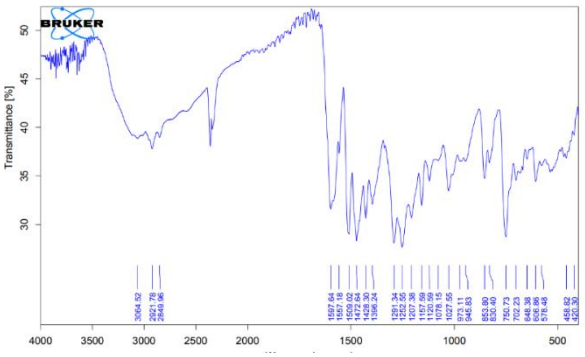

Figure (8) IR spectra of Cu Complex

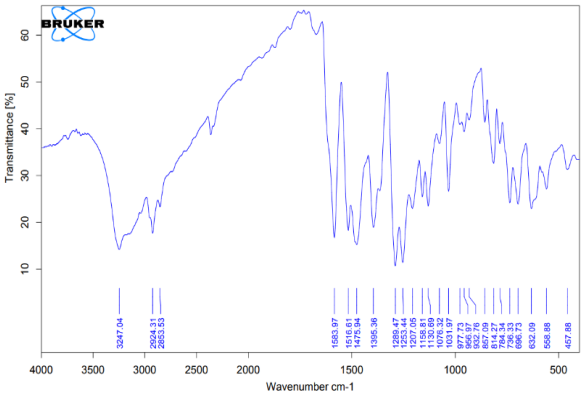

Figure (9) IR spectra of Ni Complex

CHN Analysis

Measurements of element analyses appear according to the following table:

Table (3) CHN measurement

Num.	The Elements	theoretical measurements	Practical measurements
1	carbon	58.89 %	54.82 %
2	hydrogen	4.32 %	4.18 %
3	oxygen	17.17 %	15.87 %

Electrostatic potential (MEP) Molecular

The optimization structure of the ligand was drawn by the hyper-chem program and found the electrostatic potential which is considered important to find the active site in the free ligand as shown in the figure.

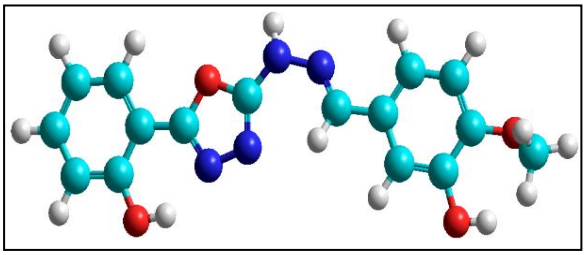

Figure (10). Graphical presentation of the stereochemistry of the Ligand (C16H14N4O4)

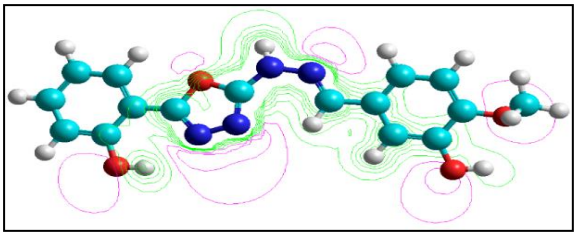

Figure (11). Electrostatic potential 2D counter of ligand

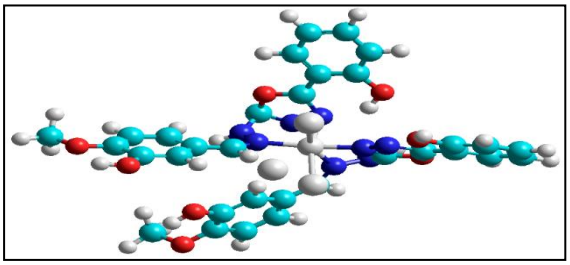

Figure (12). Graphical presentation of the stereochemistry of the [Cr(L2)Cl2]

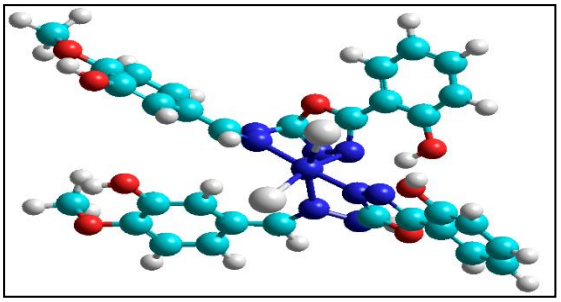

Figure (13). Graphical presentation of the stereochemistry of the [Co(L) Cl2]

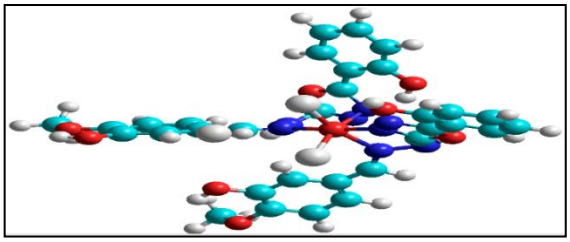

Figure (14). Graphical presentation of the stereochemistry of the [Fe (L) Cl2]

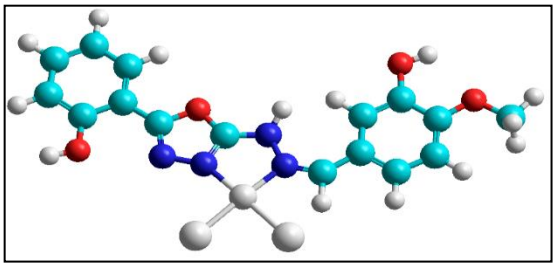

Figure (15). Graphical presentation of the stereochemistry of the [Ni (L) Cl2]

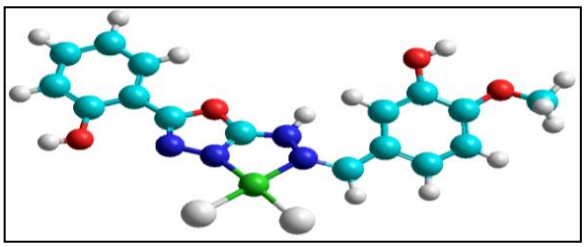

Figure (16). Graphical presentation of the stereochemistry of the [cu (L) Cl2]

Evaluation of Antioxidant Activity

The antioxidant activity of 4-({2-[5-(2-hydroxyphenyl)-1,3,4-oxadiazol-2-yl] hydrazinylidene} methyl)-2-methoxy phenol (L) A spectrophotometric approach was used to measure the antioxidant activity of 4-(2-[5-(2-hydroxyphenyl)-1,3,4-oxadiazol-2-yl] hydrazinylidene methyl)-2-methoxy phenol (L) based on a decrease in DPPH radicals at room temperature. The outcomes were contrasted with vitamin C results (Table 3). Each DPPH scavenger's ethanol solution and prepared ligand were in a concentration of 1 mM. Then, 1 ml of the DPPH solution was mixed with (0.5, 1, 2) ml of the purity ligand solution to create a new concentration of (12.5 ,25, 50,100, 200, 400) M. After (0, 1, 2) hours, absorption was measured for each solution at 516 nm. The NH and OH group transfer the hydrogen atom to the free radical to make it a stable free radical by the HAT process, which results in the ligand having high antioxidant activity. The degree of delocalization increases this stability, and the IC50 (ligand concentration needed to reduce the absorbance of the DPPH control solution by 50%) was found. The IC50 decreases as the duration and solution concentration are increased (34). Figure (17) and Table (4).
Free oxadiazole ligand antioxidant activity and IC50 values when used with DPPH radicals (standard deviation (Sd) obtained from studies performed in triplicate).

Table (4) Antioxidant activity of the ligand

Compare each cell mean with the other cell mean in that row						
Number of families	1					
Number of comparisons per family	5					
Alpha	0.05					
Sadik's multiple comparisons tests	Mean Diff.	95.00% CI of diff.	Below threshold?	Summary	Adjusted P Value	
ascorbic acid - L2						
200	4.398	-6.526 to 15.32	No	ns	0.7884	
100	8.758	-2.166 to 19.68	No	ns	0.1595	
50	0.000	-10.92 to 10.92	No	ns	>0.9999	
25	3.472	-7.452 to 14.40	No	ns	0.9069	
12.5	0.2317	-10.69 to 11.16	No	ns	>0.9999	
Test details	Mean one	Mean two	Mean Diff.	SE of diff.	N1	N 2
ascorbic acid - L2						
200	79.98	75.58	4.398	3.852	3	3
100	72.18	63.43	8.758	3.852	3	3
50	54.48	54.48	0.000	3.852	3	3
25	40.43	36.96	3.472	3.852	3	3
12.5	17.63	17.40	0.2317	3.852	3	3

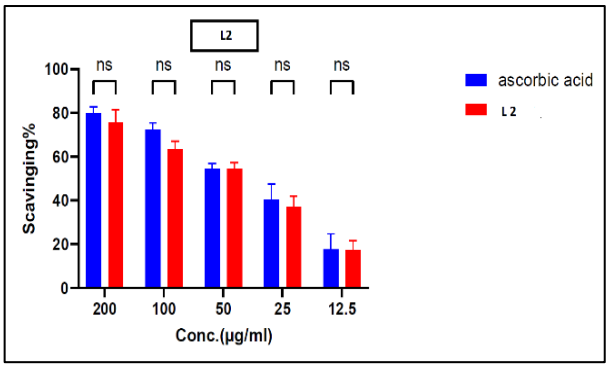

Figure (17) Antioxidant activity

Conclusion

The ligand 4-({2-[5-(2-hydroxyphenyl)-1,3,4-oxadiazol-2-yl] hydrazinylidene} methyl)-2-methoxy phenol the spectroscopic data display the involvement of CH=N groups in coordination to the central transition metal ion. The molar conductance confirms that all the complexes are non-electrolytes, just the Cr complex is the electrolyte. According to hyper chem characterization of transition metal complexes shown that octahedral geometry for Fe (III), Cr (III), tetrahedral geometry for Cu (II), Co (II), and square planar geometry was suggested for Ni (II). (L) was successfully synthesized. It acts like a bidentate ligand.

References

Katritzky, Alan R., et al. Handbook of heterocyclic chemistry. Elsevier, 2010

De Oliveira, Cledualdo Soares, et al. "Synthetic approaches and pharmacological activity of 1, 3, 4-oxadiazoles:
a review of the literature from 2000−2012 ". Molecules 17.9 (2012): 10192-10231.

Dewangan, Dhansay, et al. "Synthesis, characterization, and screening for analgesic and anti-inflammatory
activities of new 1, 3, 4-oxadiazole derivatives linked to the quinazoline-4-one ring." Medicinal Chemistry
Research 25.10 (2016): 2143-2154.

Kaya, Betьl, et al. "Design and Synthesis of New 1, 3, 4-Oxadiazole−Benzothiazole and Hydrazone Derivatives
as Promising Chemotherapeutic Agents." Drug research 67.05 (2017): 275-282.

Chen, Ling, et al. "Antiviral and Antibacterial Activities of N-(4-Substituted phenyl) Acetamide Derivatives
Bearing 1, 3, 4-Oxadiazole Moiety." Chinese Journal of Chemistry 34.12 (2016): 1236-1244.

Tiwari, Amit, et al. "Synthesis and evaluation of selected 1, 3, 4-oxadiazole derivatives for in vitro cytotoxicity
and in vivo anti-tumor activity." Cytotechnology 68.6 (2016): 2553-2565.

Ilangovan, Andivelu, Shanmugasundar Saravanakumar, and Siddappa Umesh. "T3P as an efficient
cyclodehydration reagent for the one-pot synthesis of 2-amino-1, 3, 4-oxadiazoles." Journal of Chemical
Sciences 127.5 (2015): 797-801.

Shaikh, Ambareen, and Jyotsna S. Meshram. "Design, synthesis and pharmacological assay of novel azo
derivatives of dihydropyrimidinones." Cogent Chemistry 1.1 (2015): 1019809.

Chawla, Gita, Baby Naaz, and Anees A. Siddiqui. "Exploring 1, 3, 4-oxadiazole scaffold for anti-inflammatory
and analgesic activities: a review of literature from 2005-2016." Mini reviews in medicinal chemistry 18.3
(2018): 216-233.

Shingalapur, Ramya V., et al. "Derivatives of benzimidazole pharmacophore: Synthesis, anticonvulsant,
antidiabetic and DNA cleavage studies." European Journal of medicinal chemistry 45.5 (2010): 1753-1759.

Zachariah, Subin Mary, et al. "A review on oxadiazole." Research Journal of Pharmaceutical, Biological
andChemical Sciences 6.2 (2015): 205-219.

Jayashankar, B., et al. "Synthesis and pharmacological evaluation of 1, 3, 4-oxadiazole bearing bis
(heterocycle) derivatives as anti-inflammatory and analgesic agents." European Journal of Medicinal
Chemistry 44.10 (2009): 3898-3902.

Cena, Clara, et al. "Use of the furoxan (1, 2, 5-oxadiazole 2-oxide) system in the design of new NO-donor
antioxidant hybrids." Arkivoc 7 :(2006) 301-309.

Holla, B. Shivarama, et al. "Synthesis and anticancer activity studies on some 2-chloro-1, 4-bis-(5-
substituted-1, 3, 4-oxadiazol-2-ylmethyleneoxy) phenylene derivatives ". .(2005)
El-Sayed, Wael A., et al. "Anti-HIV activity of new substituted 1, 3, 4-oxadiazole derivatives and their acyclic
nucleoside analogs." Zeitschrift fьr Naturforschung C 64.11-12 (2009): 773-778.
Husain, Asif, and Mohammed Ajmal. "Synthesis of novel 1, 3, 4-oxadiazole derivatives and their biological
properties." Acta Pharmaceutica 59.2 (:(2009 .233-223
Wang, Pei-Yi, et al. "Potent antibacterial agents: pyridinium-functionalized amphiphiles bearing 1, 3, 4-
oxadiazole scaffolds." Chemical Papers 71.6 .1018-1013 :(2017)
Katea, Azhar H. "Synthesis, Characterization, Antimicrobial New 2, 2'-[(1E, 2E)-ethane-1, 2-diylidenedi (2E)
hydrazin-1-yl-2-ylidene] bis (5-methyl1-4 ,3 , oxadiazole) and their transition metal complexes." University of
Thi-Qar Journal of Science 6.2 (2017): 1-18.
Zhang, Teng-Teng, et al. "Antibacterial and Antifungal Activities of 2-(substituted ether)-5-(1-phenyl-5-
(trifluoromethyl)-1H-pyrazol-4-yl)-1, 3, 4-oxadiazole Derivatives." Journal of Heterocyclic Chemistry 54.4
(2017): 2319-2325.
Agarwal, Mohit, et al. "Design and synthesis of new 2, 5-disubstituted-1, 3, 4-oxadiazole analogs as
anticancer agents." Medicinal Chemistry Research 25.10 (2016): 2289-2303.
Siddiqui, Nadeem, et al. "Substituted phenyl containing 1, 3, 4-oxadiazole-2-yl-but-2-enamides: synthesis
and preliminary evaluation as promising anticonvulsants." Medicinal Chemistry Research 23.11 (2014):
4915-4925.
Desai, N. C., et al. "Synthesis and biological evaluation of 1, 3, 4-oxadiazole bearing dihydro pyrimidines as
potential antitubercular agents." Medicinal Chemistry Research 25.2 (2016): 329-338.
DAHHAM, LAMYAA A., IBRAHIM A. FLIFEL, and ALYAA MAJID. "Synthesis, Characterization, and Anticancer
Activity Studies of New N-(5-phenyl-1, 3, 4-oxadizole-2-yl) propane hydrazide and its Transition Metal
Complexes." International Journal of Pharmaceutical Research 12.2 (2020.(
Shingalapur, Ramya V., et al. "Derivatives of benzimidazole pharmacophore: Synthesis, anticonvulsant,
antidiabetic and DNA cleavage studies." European Journal of medicinal chemistry 45.5 (2010): 1753-1759.
et al ZHOU, Gang, "Novel polyphenylenes containing phenol-substituted oxadiazole moieties as fluorescent
chemosensors for fluoride ion ". Macromolecules, pp. 2148−2153, 2005.
Anghel, Catalin, et al. "A novel 1-D coordination polymer constructed from disilver-1, 3, 4-oxadiazole nodes
and perchlorates bridges." Inorganic Chemistry Communications 76 (2017): 22-25.
Deshapande, Narahari, et al. "Synthesis and optoelectronic properties of thieno [2, 3-b] thiophene based bis
1, 3, 4-oxadiazole derivatives as blue fluorescent material for use in organic light-emitting diodes." Optical
Materials 37 (2014): 516-519.
Bentiss, F., M. Traisnel, and M. Lagrenee. "The substituted 1, 3, 4-oxadiazoles: a new class of corrosion
inhibitors of mild steel in acidic media." Corrosion Science 42.1 (2000): 127-146.
Era, Masanao, et al. "Double-heterostructure electroluminescent device with cyanine-dye bimolecular layer
as an emitter." Chemical physics letters 178.5-6 (1991): 488-490.
Jha, Keshari Kishore, et al. "Design, synthesis and biological evaluation of 1, 3, 4-oxadiazole derivatives."
European Journal of medicinal chemistry 45.11 (2010): 4963-4967.
Abdel-Aal, Mohammed T., et al. "Synthesis and Antiviral Evaluation of Novel 5-(N-Aryl-aminomethyl-1, 3, 4-
oxadiazol-2-yl) hydrazines and Their Sugars, 1, 2, 4-Triazoles, Tetrazoles and Pyrazolyl Derivatives." Archiv der

Pharmazie: An International Journal Pharmaceutical and Medicinal Chemistry 341.5 (2008): 307-313.
Khorshidifard, Mahsa, et al. "Cobalt (II), copper (II), zinc (II) and palladium (II) Schiff base complexes:
Synthesis, characterization, and catalytic performance in selective oxidation of sulfides using hydrogen
peroxide under solvent-free conditions." Polyhedron 95 (2015): 1-13.
Ali, A. H. K. S. A., & Flifel, I. A. (2017). Synthesis, Characterization, Antimicrobial New 2, 2'-[(1E, 2E)-ethane-
1, 2-diylidenedi (2E) hydrazin-1-yl-2-ylidene] bis (5-methyl-1, 3, 4-oxadiazole) and their transition metal
complexes.
Nazarbahjat, Nafal, et al. "Synthesis, characterization, drug-likeness properties and determination of the in
vitro antioxidant and cytotoxic activities of new 1, 3, 4-oxadiazole derivatives." Medicinal Chemistry Research
(2016): 2015-2029.
Shakir, Raied M., Azhar Ariffin, and Mahmood Ameen Abdulla. "Synthesis of new 2, 5-di-substituted 1, 3, 4-
oxadiazoles bearing 2, 6-di-tertbutylphenol moieties and evaluation of their antioxidant activity." Molecules 19.3 (2014): 3436-3449.
Saleh, M. M., Jalil, A. T., Abdulkereem, R. A., & Suleiman, A. A. Evaluation of Immunoglobulins, CD4/CD8 T
Lymphocyte Ratio and Interleukin-6 in COVID-19 Patients. TURKISH JOURNAL of IMMUNOLOGY, 8(3), 129-134.
Moghadasi, S., Elveny, M., Rahman, H.S. et al. A paradigm shift in cell-free approach: the emerging role of
MSCs-derived exosomes in regenerative medicine. J Transl Med 19, 302 (2021).
https://doi.org/10.1186/s12967-021-02980-6
JALIL, A. T., DILFY, S. H., KAREVSKIY, A., & NAJAH, N. (2020). Viral Hepatitis in Dhi-Qar Province: Demographics
and Hematological Characteristics of Patients. International Journal of Pharmaceutical Research, 12.(1)
Dilfy, S. H., Hanawi, M. J., Al-bideri, A. W., & Jalil, A. T. (2020). Determination of the Chemical Composition of
Cultivated Mushrooms in Iraq with Spectrophotometrically and High-Performance Liquid Chromatographic.
Journal of Green Engineering, 10, 6200-6216.
Jalil, A. T., Al-Khafaji, A. H. D., Karevskiy, A., Dilfy, S. H., & Hanan, Z. K. (2021). Polymerase chain reaction
technique for molecular detection of HPV16 infections among women with cervical cancer in Dhi-Qar
Province. Materials Today: Proceedings.
Marofi, F., F. Abdul-Rasheed, O., Sulaiman Rahman, H., Setia Budi, H., Jalil, A. T., Valerievich Yumashev, A., ... &
Jarahian, M. (2021). CAR-NK cell in cancer immunotherapy; A promising frontier. Cancer Science.
Widjaja, G., Jalil, A. T., Rahman, H. S., Abdelbasset, W. K., Bokov, D. O., Suksatan, W., ... & Ahmadi, M. (2021).
Humoral Immune mechanisms involved in protective and pathological immunity during COVID-19. Human
Immunology.
Jalil, A.T., Kadhum, W.R., Faryad Khan , M.U. et al. Cancer stages and demographical study of HPV16 in gene
L2 isolated from cervical cancer in Dhi-Qar province, Iraq. Appl Nanosci (2021).
https://doi.org/10.1007/s13204-021-01947-9
Sarjito, I., Elveny, M., Jalil, A. T., Davarpanah, A., Alfakeer, M., Bahajjaj, A. A. A., & Ouladsmane, M. (2021).
CFD-based simulation to reduce greenhouse gas emissions from industrial plants. International Journal of
Chemical Reactor Engineering.
Turki Jalil, A., Hussain Dilfy, S., Oudah Meza, S., Aravindhan, S., M Kadhim, M., & M Aljeboree, A. (2021).
CuO/ZrO2 Nanocomposites: Facile Synthesis, Characterization, and Photocatalytic Degradation of
Tetracycline Antibiotic. Journal of Nanostructures.
Hanan, Z. K., Saleh, M. B., Mezal, E. H., & Jalil, A. T. (2021). Detection of human genetic variation in VAC14
gene by ARMA-PCR technique and relation with typhoid fever infection in patients with gallbladder diseases in Thi-Qar province/Iraq. Materials Today: Proceedings.

Vakili-Samiani, S., Jalil, A. T., Abdelbasset, W. K., Yumashev, A. V., Karpisheh, V., Jalali, P., ... & Jadidi-Niaragh,
F. (2021). Targeting Wee1 kinase as a therapeutic approach in Hematological Malignancies. DNA Repair,
103203.
NGAFWAN, N., RASYID, H., ABOOD, E. S., ABDELBASSET, W. K., Al-SHAWI, S. G., BOKOV, D., & JALIL, A. T.
(2021). Study on novel fluorescent carbon nanomaterials in food analysis. Food Science and Technology.
Marofi, F., Rahman, H. S., Al-Obaidi, Z. M. J., Jalil, A. T., Abdelbasset, W. K., Suksatan, W., ... & Jarahian, M.
(2021). Novel CAR T therapy is a ray of hope in the treatment of seriously ill AML patients. Stem Cell
Research & Therapy, 12(1), 1-23.
Jalil, A. T., Shanshool , M. T. ., Dilfy, S. H. ., Saleh, M. M., & Suleiman, A. A. . (2021). HEMATOLOGICAL
AND SEROLOGICAL PARAMETERS FOR THE DETECTION OF COVID-19. Journal of Microbiology, Biotechnology
And Food Sciences, e4229 . https://doi.org/10.15414/jmbfs.4229

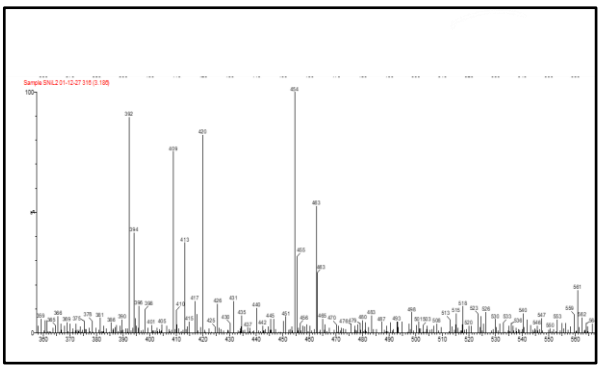

Figure (18) MS of Ni complex

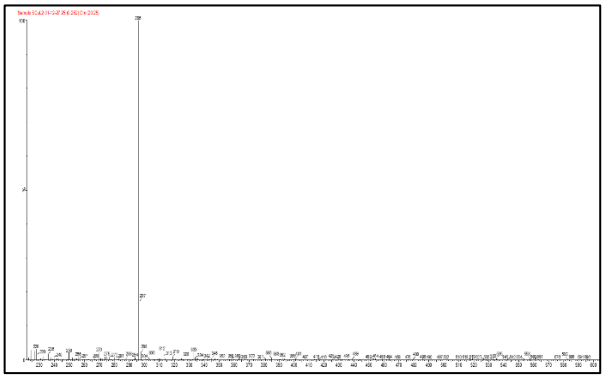

Figure (19) MS of Cu complex

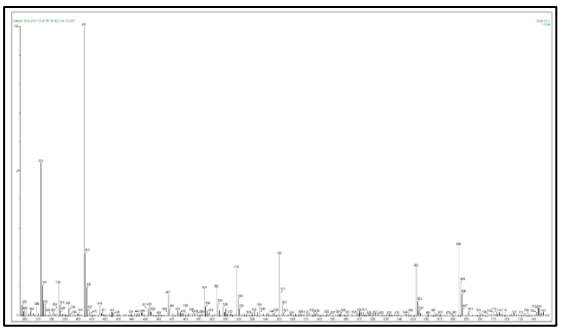

Figure (20) MS of Fe complex

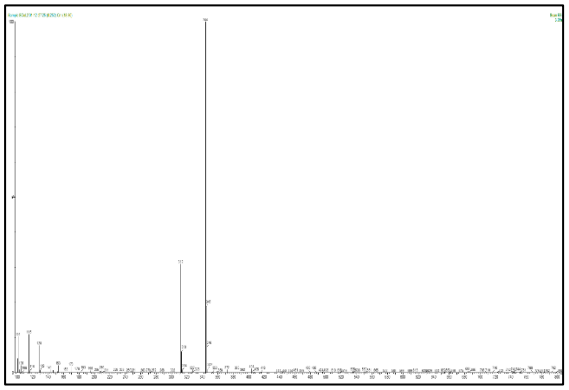

Figure (21) MS of Co complex

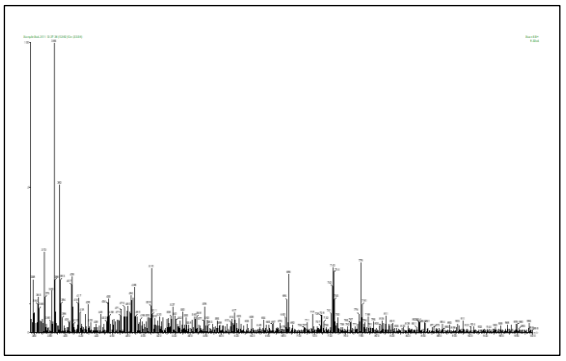

Figure (22) MS of Cr complex